Pak. j. sci. ind. res. Ser. A: phys. sci. 2014 **57**(3) 154-166

Selection of the Optimal Interpolation Method for Groundwater Observations in Lahore, Pakistan

Khalid Mahmood*, Syed Roshaan Ali, Anees Haider, Tayyab Tehseen and Shamsa Kanwal
Department of Space Science, University of the Punjab (54590), Lahore, Pakistan

(received April 15, 2013; revised September 7, 2013; accepted September 9, 2013)

Abstract. This study was carried out to find an optimum method of interpolation for the depth values of groundwater in Lahore metropolitan, Pakistan. The methods of interpolation considered in the study were inverse distance weight (IDW), spline, simple Kriging, ordinary Kriging and universal Kriging. Initial analysis of the data suggests that the data was negatively skewed with value of skewness -1.028. The condition of normality was approximated by transforming the data using a box-cox transformation with lambda value of 3.892; the skewness value reduced to -0.00079. The results indicate that simple Kriging method is optimum for interpolation of groundwater observations for the used dataset with lowest bias of 0.00997, highest correlation coefficient with value 0.9434, mean absolute error 1.95 and root mean square error 3.19 m. Smooth and uniform contours with well described central depression zone in the city, as suggested by this studies, also supports the optimised interpolation method.

Keywords: contour analysis, correlation coefficient, groundwater, interpolation, normality

Introduction

Geographical data obtained through field survey is mostly in the form of discrete measurements at regular or irregular intervals. Taking into account the cost and time, continuous measurement at every location is almost impossible. Yet, there are physical quantities that are inherently continuous in nature like temperature, water table, elevation etc. Thus, it becomes somewhat essential to know exact values of variables at every physical location. Therefore, a mechanism is required to fill in the gaps to ensure data continuity with an acceptable level of accuracy. No matter, what the method is, the process always approximates the value at un-sampled location, which can be more or less close to the exact values. Based on the degree of exactness, method selection processes can be based for better approximation. In this regard there are different possible approaches that can be used to check accuracy of the predictions. Mostly, different statistical methods and procedures are adopted to accomplish this task. The procedure of optimisation of interpolated values is a vital step as most of the further research is based on the predicted values. Therefore, selection of an optimum method becomes the key for further analysis because different interpolation methods may give different results.

A range of spatial interpolation methods are available from simple predictions to sophisticated and complex procedures (Sun *et al*., 2009). However, a uniformly optimal method for all kinds of dataset does not exist (Varouchakis and Hristopulos, 2013). Many methods have been discussed in the literature (Li and Heap, 2008). Varouchakis and Hristopulos (2013) have compared class of deterministic interpolation methods (Inverse Distance Weighted and Minimum Curvature) with Stochastic methods (ordinary Kriging and universal Kriging). Through cross-validation they have found that Stochastic methods perform well as compared to deterministic methods for groundwater interpolation.

Previous researches have been conducted by researchers around the world relating to spatial interpolation (Anderson, 2002; Caruso and Quarta, 1998). However, there is little or no harmony among the researchers on the supremacy of one technique over the other (Naoum and Tsanis, 2004). Still there are few methods that are more popular and produce best representation of the original surfaces particularly in concurrence to the field of the study of the variable. Several researches suggest that the use of geographic information system (GIS) has an advantage for studying and modeling spatial distribution of groundwater (Marchant *et al*., 2013; Rios *et al*., 2013; Sun *et al*., 2011; Thompson *et al*., 2004), however, there is no general consensus. The most commonly used methods of interpolation in geographic information systems (GIS) are inverse distance weight (IDW) (Buchanan and Triantafilis, 2009; Sun *et al*., 2009), spline (Varouchakis and Hristopulos, 2013;

*Author for correspondence; E-mail: khalid.m270@yahoo.com

Buchanan and Triantafilis, 2009) and Kriging (Pokhrel *et al*., 2013; Sun *et al*, 2009; Yang *et al*., 2008). Moreover, considerable variation within each type is also present e.g., ordinary Kriging, simple Kriging, universal Kriging. For groundwater observations, Kriging method is mostly found to be the best representing surface (Varouchakis and Hristopulos, 2013; Uyan and Cay 2013; Nikroo *et al*. 2010; Sun *et al*., 2009; Theodossiou and Latinopoulos, 2006). Kriging method have used for the interpolation of groundwater measurements and then used cross-validation for their results to check quality of the used method (Theodossiou and Latinopoulos, 2006).

Interpolation techniques. ***Inverse distance weight (IDW).*** One of the oldest spatial prediction techniques is inverse distance interpolation (Hengl, 2007), which inherently employs Tobler's law of geography (Tobler, 1970) and assumes that things that are closer together are more related.

$$z_o = \frac{\sum_{i=1}^{n} z_i \frac{1}{d^{p}{}_i}}{\sum_{i=1}^{n} \frac{1}{d^{p}{}_i}}$$

where:

z_o is the estimated value, and different choices of power p_i will result in different estimates.

Spline. Spline estimates values in order to minimise overall surface curvature, thus, it is also called minimum curvature technique. The minimum curvature (MC) method is based on Green's function, g_m, of the biharmonic equation, which satisfies $\nabla^4 g_m(s - s') = \partial(s - s')$,

where:

$\partial(s - s')$ is the Dirac delta function, the 2D Green's function is given by $g_m(d) = d^2(\ln d\text{-}1)$ (Varouchakis and Hristopulos, 2013). The MC estimate is expressed as:

$$z(s_o) = \sum_{i=1}^{N} w_i \, g_m \, (d_{i,j})$$

The weights w_i are determined by solving the following linear system at the N number of sample locations.

$$z(s_j) = \sum_{i=1}^{N} w_i \, g_m \, (d_{i,j})$$

where:

$_{i=1}$, N and $d_{i,j}$ are the distances between the sample points $d_{i,j} - |s_i\text{-}s_i|$.

Kriging. Kriging unlike IDW and spline is Stochastic and uses spatial and statistical relationships to estimate values. There are more decisions to be made regarding the spatial structure of the data like calculations of variogram parameters, variogram model, anisotropy etc., and hence it requires more input from the user. Kriging along with prediction surface also gives an error surface. It is the best linear unbiased method that depends upon spatial relationships in a dataset (Christakos, 2000; Goovaerts, 1997; Kitanidis, 1997; Isaaks and Srivastava, 1989).

All Kriging estimators are modifications of basic linear regression estimator Z*(s) defined as:

$$Z^*(s) - m(s) = \sum_{i=1}^{n} \lambda_i [Z(s_i) - m(s_i)]$$

where:

s, si = location for estimation point and neighbouring points i; n = number of data points in local neighbourhood used for estimation; m(s), $m(s_i)$ = mean global and local; λ_i = Kriging weight

Ordinary Kriging. It is a simple and commonly used type of Kriging, in which mean is assumed to be unknown. In this case the Kriging estimator can be written as:

$$Z^*(u) = m(u) + \sum_{\alpha=1}^{n(u)} \lambda_\alpha(u)[Z(u_\alpha) - m(u)]$$

$$= \sum_{\alpha=1}^{n(u)} \lambda_\alpha(u) Z(u_\alpha) + \left[1 - \sum_{\alpha=1}^{n(u)} \lambda_\alpha(u)\right] m(u)$$

Filtering the local mean by requiring Kriging weights sum to 1, the OK estimator becomes:

$$Z^*_{OK}(u) = \sum_{\alpha=1}^{n(u)} \lambda^{OK}_\alpha(u) Z(u_\alpha) \text{ with } \sum_{\alpha=1}^{n(u)} \lambda^{OK}_\alpha(u) = 1$$

Simple Kriging. In simple Kriging it is assumed that the trend component is a constant and mean, m(u), is known therefore:

$$Z^*_{SK}(u) = m + \sum_{\alpha=1}^{n(u)} \lambda^{SK}_\alpha(u) [Z(u_\alpha) - m]$$

The estimate is automatically unbiased, since E[Z(u)-m]=0. The estimation error is a linear combination of random variables representing residuals at the data points, and the estimation point.

$$Z^*_{SK}(u) - Z(u) = [Z^*_{SK}(u) - m] - [Z(u) - m]$$
$$= \sum_{\alpha=1}^{n(u)} \lambda_\alpha^{SK}(u) R(u_\alpha) - R(u) = R^*_{SK}(u) - R(u)$$

Universal Kriging. It assumes the model:

$$Z(u) = m(u) + \varepsilon(u)$$

where:

m(u) is some deterministic function Trend can also be composed of a linear function of the spatial coordinates themselves. The universal Kriging types assume that there is a structural component present and that the local trend varies from one location to another. Trends that vary, and where, the regression coefficients are unknown, form models for universal Kriging.

Variography. It is to fit a spatial-dependence model to data for quantifying the spatial-dependence. Kriging uses the model fitted from variography to make predictions. The empirical variogram provides a description of how the data are correlated with distance.

If there are no distinct anisotropy, the omnidirectional empirical semivariogram is estimated, otherwise, directional variograms are used. Mathematically it is given as:

$$\gamma(r) = \frac{1}{2N(r)} \sum_{i=1}^{N(r)} \{z(s_i - z(s_i + r))^2\}$$

where:

γ(r) = semivariogram; N(r) is the number of pairs at lag r (Varouchakis and Hristopulos, 2013). Variograms constructed from the sample do not give semivariances for all of separation distances then it is necessary to model the variograms for all possible values of separation distances. Some variogram models reach the sill, while others do not. Transition models are those that reach a plateau. The plateau is the sill, and the corresponding lag distance is the range.

Circular model. A circular semivariogram model is based on 2D geometry and is valid in 2 or 1 dimensions. Mathematically it is given as:

$$\gamma(r) = c_o + c\,(1 - \frac{2}{\pi}\cos^{-1}\frac{h}{a} + \sqrt{1 - \frac{h^2}{a^2}}$$

Spherical model. It is given as:

$$\gamma(r) = \begin{cases} 1.5(\frac{h}{a}) - 0.5\left(\frac{h}{a}\right)^3 & \text{if } h \le a \\ 1 & \end{cases}$$

Near 0, it has a linear behaviour for small h but flattens out at greater h, and attains the sill at a.

The Exponential model. Mathematically it is described as:

$$\gamma(r) = 1 - \exp(-\frac{3h}{a})$$

Near 0, it is linear for small h, but it rises more steeply and then flattens out more gradually than the spherical model. It reaches its sill asymptotically. Its practical range, a, corresponds to 95% of the sill.

The Gaussian model. It is used to model extremely continuous phenomena:

$$\gamma(r) = 1 - \exp(-\frac{3h^2}{a^2})$$

Its practical range also corresponds to 95% of the sill as it reaches its sill asymptotically.

In this paper all four discussed interpolation methods for subclasses of Kriging are analysed and compared to optimise the better prediction method for dataset in hand. Further, this optimisation is verified by groundwater hydrology studies of the area using contour patterns as an indicator of the underlying aquifer type.

Materials and Methods

Static water level values for the months of April, July and October 2011, were available from water and sanitation agency (WASA). WASA periodically measures the depth on each of its tubewells installed within Lahore district. However, in each month observation, values for all of its installed tubewells is not noted. The sampling locations are unevenly distributed and the presence of river Ravi on the NE side has a profound effect on the depth values.

The coordinate information for 476 tubewells was gathered by field survey of each tubewell site using Garmin GPSmap 76CSx with an accuracy of 3 meter, shown in Fig. 1. The depth values for October 2011, are selected for the work as it was the most recent data available.

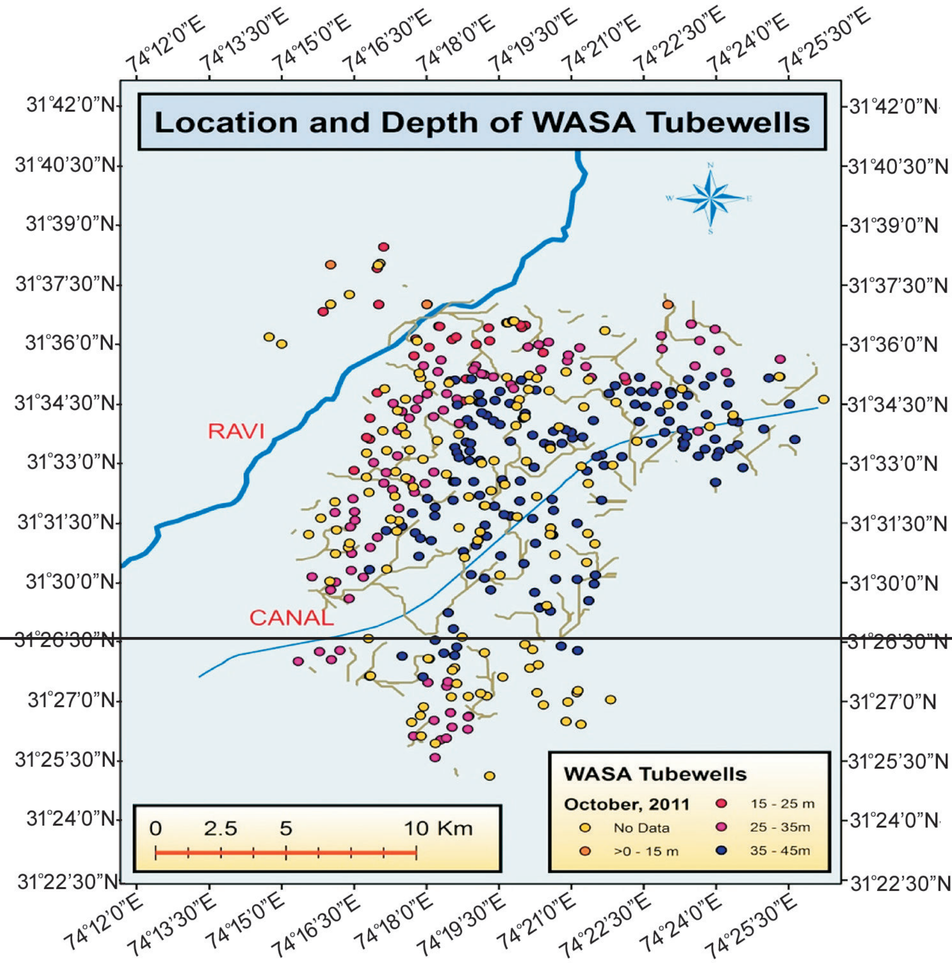

Fig. 1. Distribution of tubewell locations with surface hydrologic setup.

The data of October 2011 has 291 recorded observations, the statistical summary of the samples is given in Table 1.

The data was negatively skewed -1.028 and the statistical test of Shapiro-Wilk suggests that the data in its original form cannot be approximated to a normal distribution. However, using a box-cox transform of lambda value of 3.85, the skewness value reduces to -0.00079. The data can then be approximated by a normal distribution as shown in Fig. 2.

The 3D projection of the data values suggests that there is a global trend in the data. This information becomes useful during universal Kriging to detrend the data.

Statistical parameters used for demonstration of efficiency. The following utilities and parameters are used to perform comparison of the interpolation methods in this study.

Cross-validation. This process iteratively removed an observation from the dataset and estimated the value at that point using the remaining values (Arlot and Celisse,

Table 1. Initial statistics of the data

Mean	5% Trimmed mean	Median	Variance	SD	Minimum	Maximum	Range	IQR	Skewness	Kurtosis
34.149	34.728	36.45	58.921	7.676008	9.12	45.02	35.9	10.4	-1.028	0.468

SD = standard deviation; IQR = Interquartile range.

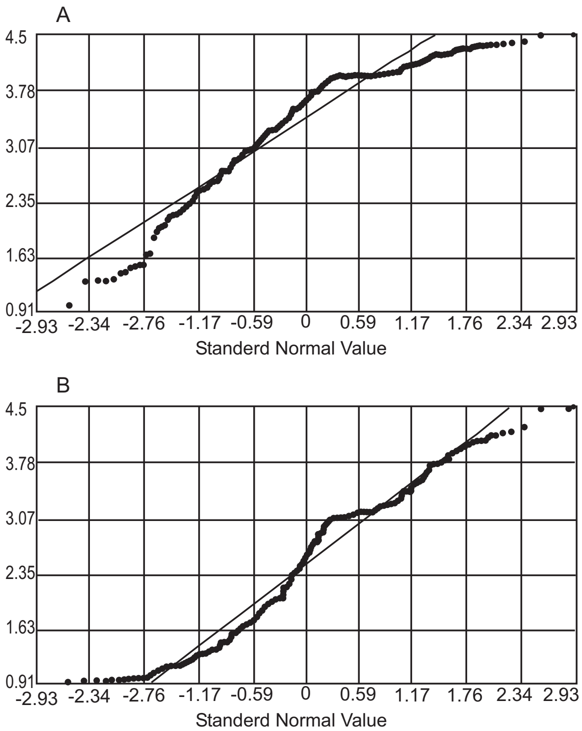

Fig. 2. Data before transformation (A) and after the box-cox 3.85 transformation (B).

2010). The estimated and the original values were then compared to calculate residuals, which were in fact the error of the surface at each location. It is the statistics performed on these errors that forms the basis of method selection procedures. Cross-validation process has been very commonly used in method selection (Sun *et al*., 2009; Theodossiou and Latinopoulos, 2006; Caruso and Quarta, 1998).

RMSE. The chief selected explanation of cross-validation is root mean squared error (RMSE) (Sun *et al*., 2009). It can cope for stationary points and extremes, and is calculated as:

$$\text{RMSE} = \sqrt{\frac{1}{n}\sum_{i=1}^{n}(Z_i - Z)^2}$$

where:

Z = estimated value; Z_i = measured values at sampling point; n = number of values used for estimation.

Bias. The mean of the error distribution is often referred to as bias and a reasonable goal for any estimation method is to produce unbiased estimates so the bias should be as close to zero as possible.

Mean absolute error (MAE). A summary statistic that incorporates both the bias and the spread, is the mean absolute error which is given:

$$\text{MAE} = \frac{1}{n}\sum_{i=1}^{n}|r|$$

Correlation. Correlation between measured and predicted values was another criterion (Sun *et al*., 2009; Caruso and Quarta, 1998) used here to assess the suitability of interpolation methods.

Error plots. The graphs drawn between the measured and the estimated values along with another graph between the error and measured values give a good indication of the areas or regions of over-prediction and under-prediction (Theodossiou and Latinopoulos, 2006).

Contour analysis. A further analysis of suitability was done using the respective contours of each type of interpolation. The roughness and smoothness of the resulting contours from different methods can be used to assess the effect of different decisions like the number of neighbours included leading to considerable variation of the estimates (Varouchakis and Hristopulos, 2013), or the smoothness due to the inherent nature of method like MC. By relating the contours with the knowledge of the local groundwater dynamics of the region, a discussion on the suitability of the contours can be done.

Analysis of uncertainty. Numerous quantitative measures can be used as a goodness-of-fit statistic for the variograms. The standard deviation of the estimation error is an index of uncertainty based on the number of nearby data points, the proximity of the samples, and also the interaction between the various factors (Sun *et al*., 2009).

Method adopted for the study. The interpolations performed were IDW, spline, ordinary Kriging, simple Kriging and universal Kriging. ArcGIS 9.3 software was used for this purpose. Each type of interpolation was performed on October 2011 depth values without forming subsets of the data.

Deterministic methods. For IDW, the decisions to be made were of the power value which was optimised and the optimum value calculated was 2. The shape of the neighbourhood is specified and constraints within the shape are established. An anisotropy factor of 1.25 was used with semi- major axis of 1000 m and semi-minor axis was 800 m. The direction was at 20°. Neighbour search was done using eight sectored ellipse with a minimum of 2 points in each sector and a maximum of 5 points. This was done to ensure that the neighbours selected were from all sides and not only one.

For spline, the sub-method used from the available methods was the 'completely regularized spline' which is the common minimum curvature method. Like IDW, to incorporate the directionality of the data as shown in Fig. 3, the direction was taken as 20° and the major axis was 1000 m with minor axis of 800 m.

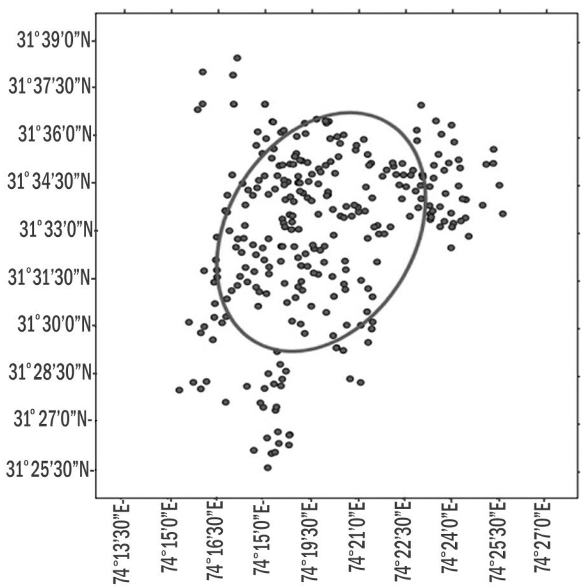

Fig. 3. Directional distribution, standard deviational ellipse (1 SD).

Stochastic methods. For using Kriging family of interpolators, variograms are constructed and different classical models like spherical, exponential and Gaussian are fit on the data. The semivariograms are constructed using the method of moments. Parameters like the correlation length and sill are calculated for each fitted model. The selection of the optimal semivariogram model was done using leave one out cross-validation. The pattern of the data appears relatively isotropic with its major axis aligned in the NE direction. The directional variograms shown in Fig. 4, give a clear indication that the presence of river Ravi on the north-western side gives a directionality to the data with axis of maximum continuity at an angle of 45° and the axis of small scale variability at an angle of 130° as shown in Fig. 4.

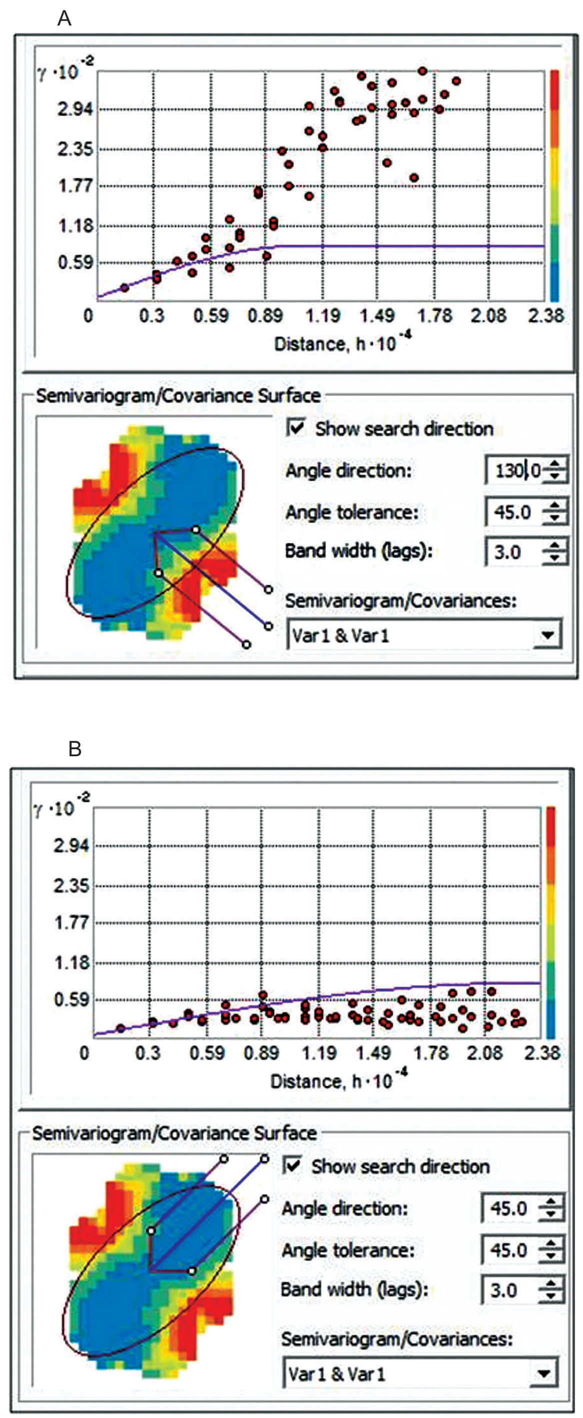

Fig. 4. Anisotropic behaviour at 130° (A) and at 45° (B) in two different direction.

Anisotropic models are fit to the data to cater for this directionality and the neighbourhood searches are thus elliptical. The 'neighbours to include' were chosen based on the range and correlation lengths obtained from variogram models.

For universal Kriging the first order 90-100% global detrending was done to obtain the optimum results. The trend in the data was evident in Fig. 5. Moreover, 100% global second order detrending also produced better results.

Semivariogram model parameters are calculated using least squares method applied to the data. Table 2, lists the optimal estimates of the parameters of the variogram models used in this study.

In most cases 11 neighbours with minimum of 4 neighbours were selected and produced the best results in terms of RMSE, R, MAE for the respective model.

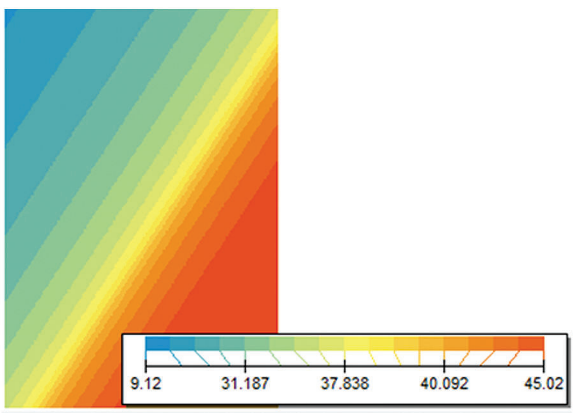

Fig. 5. Global trend in the data used in universal Kriging.

Table 2. Optimal estimates of semivariogram model parameters obtained through least square fit

Method	Partial sill	Nugget	Major range (m)	Anisotropy factor	Direction
Ok-Sp	78.924	5.7	22578	2.1384	46.3°
Ok-Ex	80.017	0	22639	1.9629	46.5°
Ok-Ga	80,687	14.504	22585	2.3713	46.2°
Sk-Ci	81.242	5.6289	12322	1.2	48.6°
Sk-Sp	83.297	5.3551	14475	1.3	49.3°
Sk-Ex	81.72	0	15176	1.5	48.5°
Sk-Ga	68.9	12.264	14668	1.6	48.6°
Uk-Ci	25.375	9.346	8887	1.05	85.6°
Uk-Sp	26	8.907	10073	1.08	84.4°
Uk-Ex	31.112	5.634	12569	1.3	84.8°
Uk-Ga	24.343	13.2	12457	1.5	85.2°

Results and Discussion

The surfaces appreciably differ among various methods so it is rather difficult to decide on a good interpolation method only by observing the corresponding surfaces. Table 3 compares all the interpolation methods selected for this study, the results show that the family of stochastic methods are better as compared to deterministic methods. Among stochastic, simple Kriging using Gaussian model (Sk-Ga) with lowest values of bias and mean absolute error and highest correlation coefficient can be ranked at first place in the ranking of optimal methods for current dataset. Universal Kriging using Gaussian model (Uk-Ga) has also shown good values for the measured parameters and may be ranked at second place in the ranking of optimal methods. Universal Kriging with spherical model (Uk-Sp) is also good but have higher bias as compared to the other two. This result is coherent with various previous studies which found Kriging to be the optimal method for groundwater observations (Varouchakis and Hristopulos 2013; Sun *et al*., 2009; Theodossiou and Latinopoulos, 2006; Naoum and Tsanis, 2004; Anderson, 2000).

Error-plots. Table 4 shows the error-plots depicting the areas of over-prediction and under-prediction. In measured *versus* predicted graphs, the grey-dotted line

Table 3. Statistical results for efficiency of different Interpolation methods for used dataset

Method	Bias	RMSE	MAE	ASE	RMSSE (m)	R
IDW	0.02623	3.418	2.0443	N/A	N/A	0.895078
Spline	0.0513	3.341	2.0262	N/A	N/A	0.892455
Ok-Ci	0.03.00	3.336	1.999	3.49	0.975	0.900345
Ok-Sp	0.03878	3.350	1.994	3.324	1.041	0.89953
Ok-Ex	0.02825	3.857	2.194	2.69	2.999	0.868337
Ok-Ga	-0.1336	3.288	2.090	3.942	0.8326	0.90354
Sk-Ci	0.04673	3.357	1.994	3.368	1.029	0.89914
Sk-Sp	0.0485	3.363	1.996	3.339	1.045	0.898744
Sk-Ex	0.0363	3.800	2.192	2.811	3.111	0.871576
Sk-Ga	0.00997	3.190	1.95	3.216	0.961	0.94340
Uk-Ci	-0.07075	3.280	2.059	3.586	0.8963	0.90900
Uk-Sp	-0.0925	3.224	2.010	3.35	0.912	0.91700
Uk-Ex	-0.06617	3.292	2.097	3.291	1.034	0.90340
Uk-Ga	-0.0652	3.212	1.971	3.353	0.939	0.92840

RMSE = root mean square error; MAE = mean absolute error; ASE = average standard error; RMSSE = root mean square standardised; R = correlation coefficient; Ok = ordinary Kriging; Sk = simple Kriging; Uk = universal Kriging; Ci = circular model; Sp = spherical model; Ex = exponential model; Ga = Gaussian model.

Table 4. Table of error-plots of each interpolation method

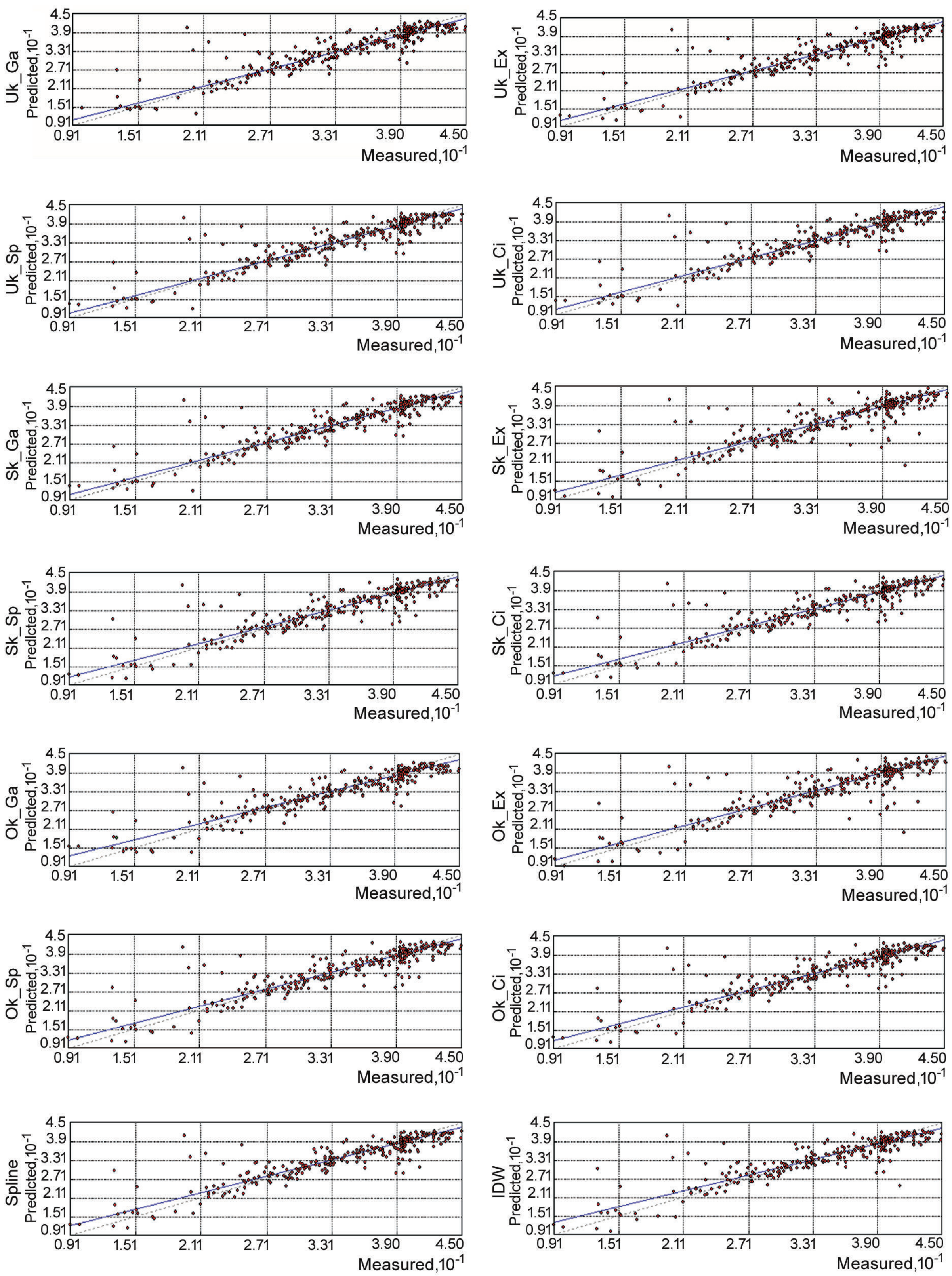

* = solid line (blue) is the trend line of the points and dotted line (grey) is zero residual line.

represents zero residuals (measured equal to predicted) and the solid blue lines represent the trend lines of the measured *versus* predicted scatter-plots. In all of these methods, the lower values are over-predicted and the higher values are under-predicted, as shown by the blue line above the grey line. The amount of over-prediction and under-prediction shown by the separation between the blue and grey lines along with the position of the zero residual point (intersection of blue and grey lines) can give a good indication of the better interpolation methods.

The intersection point of the two lines is farthest along the X-axis for IDW at about 3.31 and for spline at about 3.00. The intersection point is comparatively closer to origion along X-axis for the class of Kriging at about 2.71. Similarly, the degree of separation between the lines is greater for deterministic methods and lesser for stochastic methods. Among stochastic Sk-Ga, Uk-Sp and Uk-Ga have least separation between the lines as compared to others. The slight difference in separation of these three types is not noticeable. However, statistical results suggest that Sk-Ga lines should be slightly closer than Uk-Sp and Uk-Ga.

Contour analysis. In Fig. 6 the contours clearly demonstrate that values at locations are very much dependent upon the adopted interpolation method. IDW and spline contours are somewhat similar and have a very edgy, irregular and abruptly changing behaviour, which is not possible for an aquifer consisting primarily of different types of sand (Mahmood *et al*., 2013). Actually, the study area is underlain by unconsolidated alluvial deposits of Quaternary age and the aquifer is composed of unconsolidated alluvial complex (Basharat and Rizvi, 2011). The Lahore aquifer is unconfined alluvium with a thickness of about 400 m (1300 ft) (Mahmood *et al*., 2013; Gabriel and Khan, 2006). Despite its heterogeneity, the alluvial sediments constitute a large aquifer, which on regional basis behaves as a homogenous and highly transmissive aquifer (Gabriel and Khan, 2006). A number of studies have reported the formation of a depression zone in the central part of the study area (Mahmood *et al*., 2013). The best method of interpolation of groundwater level observations must be the one that has ability to show these declining regions more descriptively.

For IDW and spline the central contour of 42 m around the area of Shadman, Lahore, is quite edgy and has been split into two contours. The left one is more squeesed. There are no defined contours in lower right and central right portions. Not much variation is detected thereby these methods. All Kriging contours are more regular and do not have abrupt edges and turns, as expected for groundwater depth values in a region of almost similar elevation and population density (central city region). The central region of 42 m depth has a single continuous contour in case of three optimal methods (Sk-Ga, Uk-Sp and Uk-Ga). However, the existence of depression at centre of the city, surrounded by gradual rise in groundwater levels (Mahmood *et al*., 2013) has been addressed by Sk-Ga with more elaborated details.

Analysis of uncertainity. The standard deviations of the estimation errors for the different interpolation surfaces are shown in Table 5 and can be used to assess the uncertainty in the predictions. The best value is again for the simple Kriging with Gaussian model of 3.09. Uk-Ga is ranked second and Uk-Sp is ranked at third place. The median absolute deviation is a goodness of fit statistic, lesser its value, better is the fit of the model to data. The most suited values of median absolute deviation are highlighted by yellow background in Table 5.

Kriging variance. Kriging variance is the square of the Kriging standard error map. Thus the distribution of the Kriging variance throughout the predicted surface can be observed. The output variance of prediction raster contains the Kriging variance at each output raster cell. Low values within the output variance of prediction raster indicate a high degree of confidence in the predicted value. High values may indicate a need for more data points. Fig. 7 shows the distribution of the standard error and hence, the Kriging variances for the two optimal methods of this study (simple Kriging using Gaussian variogram and universal Kriging using Gaussian model). Maximum variance is observed in the lower right portion, which is highly under-sampled. Therefore, further sampling within this region can improve the prediction statistics. The most reliable estimates are in the central region of high depth values, where sampling locations are clustered together. The variance classes are elongated in the same direction of continuity as observed earlier. Overall the range of standard error surface for simple Kriging is much less than the range for the universal Kriging surface, hence, the estimates from the simple Kriging using Gaussian model are more reliable than the former.

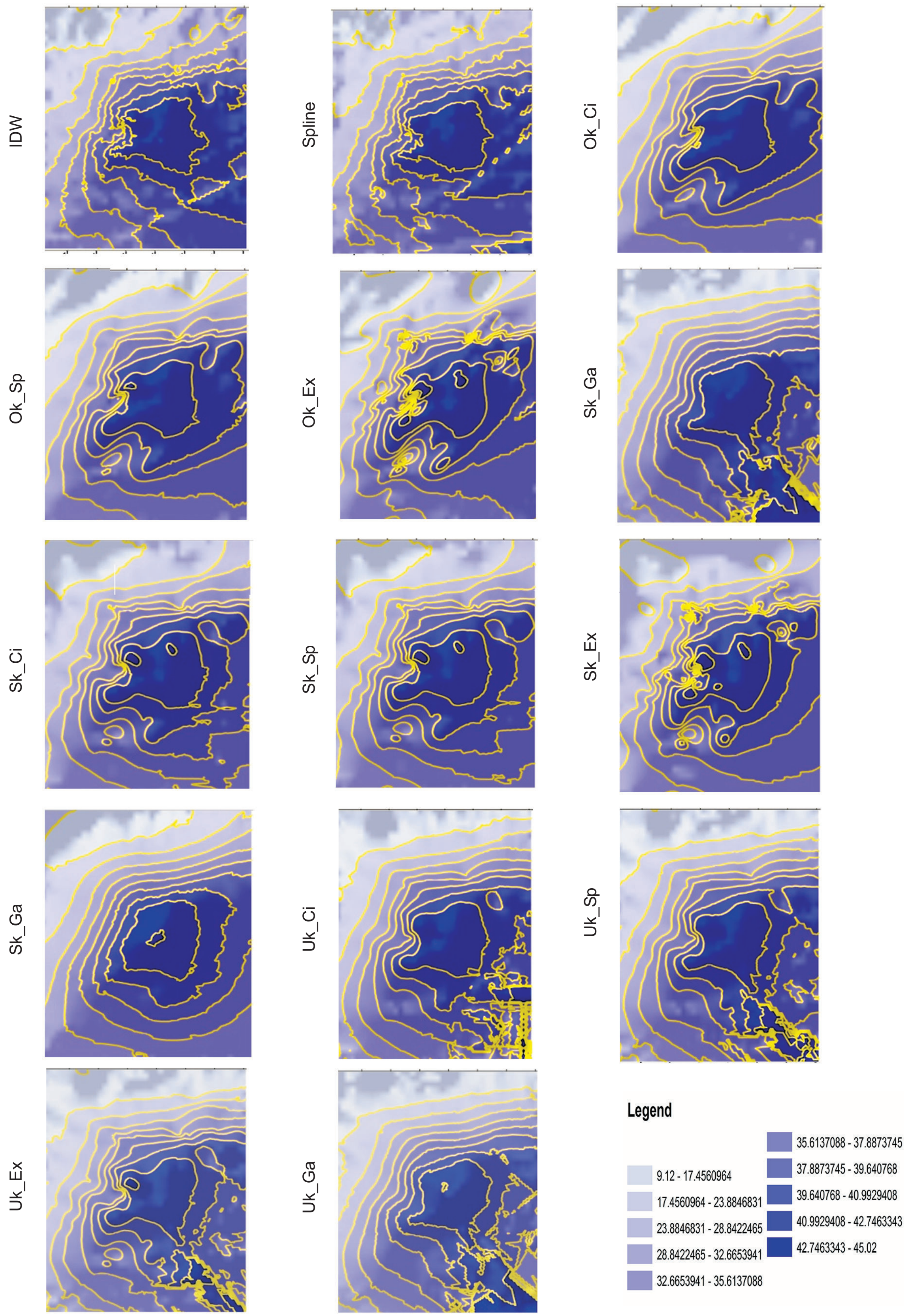

Fig. 6. Contours for the final interpolation surfaces.

Table 5. Measured values of uncertainty parameters

Method (measured *vs*.)	SD of estimation error	Median absolute deviation	Method (measured *vs*.)	SD of estimation error	Median absolute deviation
IDW	3.424	1.202	Sk_Sp	3.369	1.122
Spline	3.312	1.200	Sk_Ex	3.806	1.254
Ok_Ci	3.341	1.175	Sk_Ga	3.099	1.1
Ok_Sp	3.356	1.100	Uk_Ci	3.227	1.088
Ok_Ex	3.864	1.214	Uk_Sp	3.214	1.058
OK_Ga	3.291	1.206	Uk_Ex	3.297	1.088
Sk_Ci	3.362	1.118	Uk_Ga	3.199	1.101

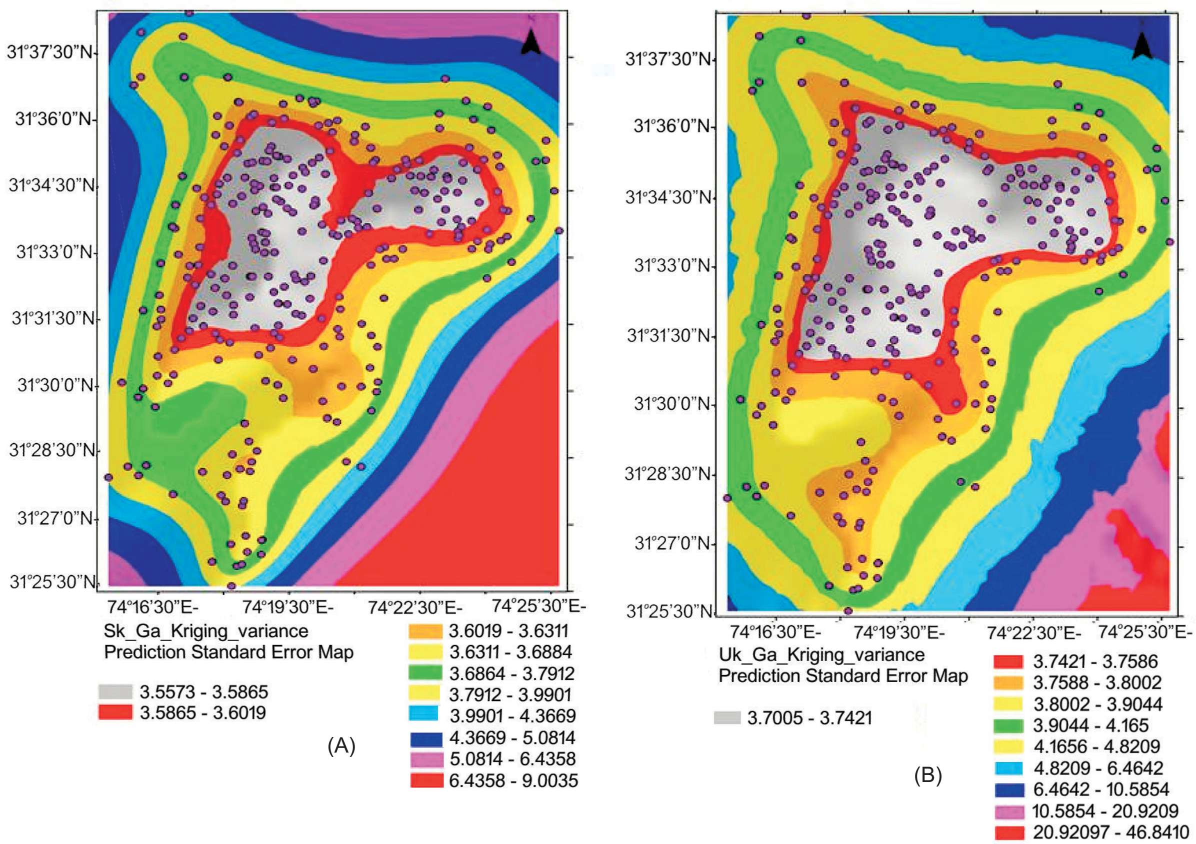

Fig. 7. Prediction standard error maps for Sk-Ga (A) and Uk-Ga (B).

Conclusion

The above analysis shows that Kriging performs better for groundwater observations. Among Kriging types, simple Kriging with Gaussian variogram model is found to be the optimal interpolation method for the datasets used in this study. However, universal Kriging with Gausian variogram model and universal Kriging with Spherical variogram model may be ranked at second and third places, respectively. It is also observed that using appropriate variogram model, stochastic methods perform better than deterministic methods. Kriging variance has clearly shown that density of sampling location has strong influence on accuracy of the predicted value at the location. This study also concludes that contour pattern analysis on the basis of known variations in the physical variable under study can also serve as a tool of optimisation of the interpolation technique.

References

Anderson, S. 2002. An evaluation of spatial interpolation methods on air temperature in phoenix, AZ. Department of Geography, Arizona State University. http://www.cobblestoneconcepts.com/ucgis2summer/anderson/anderson.htm

Arlot, S., Celisse, A. 2010. A survey of cross-validation procedures for model selection. *Statistics Surveys*, **4:** 40-79.

Basharat, M., Rizvi, S.A. 2011. Groundwater extraction and waste water disposal regulation: Is Lahore aquifer at stake with as usual approach. In: *Proceedings of Pakistan Engineering Congress, World Water Day*, pp. 112-134, http://pecongress.org.pk: on Sep. 2012.

Buchanan, S., Triantafilis, J. 2009. Mapping water table depth using geophysical and environmental variables. *Ground Water*, **47:** 80-96.

Caruso, C., Quarta, F. 1998. Interpolation methods comparison. *Computers & Mathematics With Applications*, **35:** 109-126.

Christakos, G. 2000. *Modern Spatiotemporal Geostatistics*, 234 pp., 1st edition, Oxford University Press, New York, USA.

Gabriel, H.F., Khan, S. 2006. Policy options for sustainable urban water cycle management in Lahore, Pakistan. In: *Proceedings of International ERSEC Conference on Sustainable Water Management: Problems and Solutions Under Water Scarcity*, pp. 180-202, Beijing, China.

Goovaerts, P. 1997. *Geostatistics for Natural Resources Evaluation-Applies Geostatistics Series*, pp. 127, 133, 154, Oxford University Press, New York, USA. http://books.google.com

Hengl, T. 2007. *A Practical Guide to Geostatistical Mapping of Environmental Variables*, JRC Scientific and Technical Reports 143 pp., Office for Official Publications of the European Communities, Luxembourg.

Isaaks, E.H., Srivastava, R.M. 1989. *An Introduction to Applied Geostatistics*, pp. 370-400, 1st edition, Oxford University Press, New York, USA.

Kitanidis, P.K. 1997. *Introduction to Geostatistics*: *Hydrogeology*, 77 pp., Cambridge University Press, New York, USA.

Li, J., Heap, A.D. 2008. A review of spatial interpolation methods for environmental scientists. *Geoscience Australia*, Record 2008/23, 137 pp.

Mahmood, K., Rana, A.D., Tariq, S., Kanwal, S., Ali, R., Ali, H., Tahseen, T. 2013. Groundwater levels susceptibility to degradation in Lahore Metropolitan. *Science International Lahore*, **25:** 123-126.

Marchant, A.P., Banks, V.J., Royse, K.R., Quigley, S.P. 2013. The development of a GIS methodology to assess the potential for water resource contamination due to new development in the 2012 Olympic Park site, London. *Computers & Geosciences*, **51:** 206-215.

Naoum, S., Tsanis, I.K. 2004. Ranking spatial interpolation techniques using a GIS based DSS. *Global Nest*: *The International Journal*, **6:** 1-20.

Nikroo, L., Kompani-Zare, M., Sepaskhah, A.R., Shamsi, S.R. 2010. Groundwater depth and elevation interpolation by kriging methods in Mohr Basin of Fars province in Iran. *Environment Monitoring and Assessment*, **166:** 387-407.

Pokhrel, R.M., Kuwano, J., Tachibana, S. 2013. A Kriging method of interpolation used to map liquefaction potential over alluvial ground. *Engineering Geology*, **152:** 26-37.

Rios, J.F., Ye, M., Wang, L., Lee, P.Z., Davis, H., Hick, R. 2013. ArcNLET: A GIS-based software to simulate groundwater nitrate load from septic systems to surface water bodies. *Computers & Geosciences*, **52:** 108-116.

Sun, D., Zaho, C., Wei, H., Peng, D. 2011. Simulation of the relationship between land use and groundwater level in Tailan River basin, Xinjiang, China. *Quaternary International*, **244:** 254-263.

Sun, Y., Kang, S., Li, F., Zhang, L. 2009. Comparison of interpolation methods for depth to groundwater and its temporal and spatial variations in the Minqin oasis of northwest China. *Environmental Modeling & Software*, **24:** 1163-1170.

Theodossiou, N., Latinopoulos, P. 2006. Evaluation and optimization of groundwater observation networks using the Kriging methodology. *Environmental Modeling & Software*, **21:** 991-1000.

Thompson, J.R., Refstrup, S.H., Gavin, H., Refsgaard, A. 2004. Application of the coupled MIKE SHE/MIKE II modeling system to a low land wet grass land in southeast England. *Journal of Hydrology*, **293:** 151-179.

Tobler, W.R. 1970. A computer movie simulating urban growth in the Detroit region. *Economic Geography*, **46:** 234-240.

Uyan, M., Cay, T. 2013. Spatial analyses of groundwater level differences using geostatistical modeling. *Environmental and Ecological Statistics*, **20:** 633-646.

Varouchakis, E.A., Hristopulos, D.T. 2013. Comparison of stochastic and deterministic methods for mapping groundwater level spatial variability in sparsely monitored basins. *Environmental Monitoring and Assessment*, **185:** 1-19.

Yang, F.G., Cao, S.Y., Liu, X.N., Yang, K.J. 2008. Design of groundwater level monitoring network with ordinary Kriging. *Journal of Hydrodynamics*, **20:** 339-346.